Addendum to "Optimal Parametric Design of Radial Magnetic Torque Couplers via Dimensional Analysis"

Brandon E. Carroll[1], Jacob L. B. Aman[2], Shad Roundy[1,3], and Jake J. Abbott[1,3]

[1]Department of Mechanical Engineering, The University of Utah, Salt Lake City, UT 84112 USA
[2]Lawrence Livermore National Laboratory, Livermore, CA 94550 USA
[3]Robotics Center, The University of Utah, Salt Lake City, UT 84112 USA

Radial (also known as radial-flux) magnetic torque couplers (MTCs) enable the transfer of torque between an inner rotor (IR) and an outer rotor (OR), each equipped with a set of permanent magnets. In a previous article, we used dimensional analysis to find the minimum set of nondimensional parameters required to characterize an MTC, and then performed a parametric optimization to maximize the synchronous torque (i.e., the torque required to cog the IR with respect to the OR) in a given package size. However, we only explicitly optimized an MTC with 16 IR magnets and 16 OR magnets, which results in eight stable magnetic equilibria. In this addendum, we applied the same methodology to consider MTCs with 1, 2, 4, 8, 16, and 32 stable equilibria. We observe clear trends in the optimal values of the various MTC parameters as we change the number of magnets. We also find that the maximum synchronous torque grows asymptotically with the number of stable equilibria, with a diminishing return beyond 16.

***Index Terms*— Actuators, industrial magnetism, motors, transducers.**

I. Introduction

RADIAL (also known as radial-flux) magnetic torque couplers (MTCs) are magnetic devices that transfer torque between an inner rotor (IR) and an outer rotor (OR), each equipped with a set of permanent magnets, without direct mechanical contact. An MTC can be designed to have any positive integer number of stable equilibria, Z, with an angle $\phi = 360°/Z$ between stable equilibria, by equipping the IR and OR with $2Z$ magnets each. In our previous article [1], we identified 12 independent variables that affect the maximum synchronous torque, T, of an MTC, for any given value of Z (Table I); eight of these variables are geometric (Fig. 1) and the remaining four represent the permanent-magnet (PM) material in the IR and OR magnets and the soft-magnetic (SM) material in the core and yoke. We then utilized dimensional analysis (i.e., the Buckingham Π theorem) to identify ten dimensionless Π groups, nine independent (Π_1–Π_9) and one dependent (Π_0), that can be used to fully characterize T (Table I). We then performed a parametric optimization in this nondimensional space, with the goal of maximizing the maximum synchronous torque (i.e., the torque required to cause the IR to cog with respect to the OR) within a given package size. However, we only explicitly optimized an MTC with $Z = 8$. In this addendum, we apply the methodology of [1] to optimize MTCs with $Z \in \{1, 2, 4, 8, 16, 32\}$.

II. Methods

We follow the methodology described in [1], except where noted. As in [1], we constrain some of our independent variables to practically relevant values to simplify the optimization process. For the SM material in the core and yolk, properties representing Vacoflux 50 were selected; for the magnets in the IR and OR, properties representing Grade-N45SH NdFeB were selected. These were chosen because they are representative of the type of material that would be used in a high-performance MTC. These choices result in constant properties for $\mu_y = (1.5 \times 10^4)\mu_0$, where $\mu_0 = 4\pi \times 10^{-7}$ N/A^2 is the permeability of free space, $B_y = 2.35$ N/(A·m), $\mu_m = 1.046\mu_0$, and $H_{cm} = 1.027 \times 10^6$ A/m. Holding these properties at given values means that Π_8 and Π_9 are constants and are thus not included in the

TABLE I
Parameters With Their Symbols, Units, and Respective Nondimensional Π Groups

Parameter	Symbol	Units	Π Group
Torque	T	N·m	$\Pi_0 = \frac{T}{\mu_m H_{cm}^2 R^3}$
Length	L	m	$\Pi_1 = \frac{L}{R}$
Outer Radius	R	m	·
IR Magnet Thickness	d_m	m	$\Pi_2 = \frac{d_m}{R}$
Air-gap Thickness	d_g	m	$\Pi_3 = \frac{d_g}{R}$
OR Slot Depth	d_s	m	$\Pi_4 = \frac{d_s}{R}$
Yoke Thickness	d_y	m	$\Pi_5 = \frac{d_y}{R}$
OR Slot Fraction	E	·	$\Pi_6 = E = \frac{\beta_s}{\beta_p}$
IR Magnet Fraction	F	·	$\Pi_7 = F = \frac{\alpha_m}{\alpha_p}$
SM Permeability	μ_y	$\frac{\text{N}}{\text{A}^2}$	$\Pi_8 = \frac{\mu_y}{\mu_m}$
SM Saturation	B_y	$\frac{\text{N}}{\text{A·m}}$	$\Pi_9 = \frac{B_y}{\mu_m H_{cm}}$
PM Permeability	μ_m	$\frac{\text{N}}{\text{A}^2}$	·
PM Coercivity	H_{cm}	$\frac{\text{A}}{\text{m}}$	·

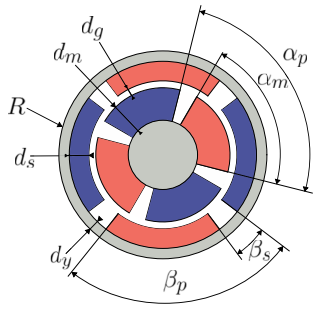

Fig. 1. Schematic of an MTC with $Z = 2$, showing definitions of independent variables. Red indicates magnetization radially outward, and blue indicates magnetization radially inward. α_p and α_m are used to calculate IR magnet fractions. β_p and β_s are used to calculate OR slot fractions.

Received 5 September 2025; revised 27 October 2025; accepted 30 October 2025. Date of publication 3 November 2025; date of current version 30 December 2025. Corresponding author: J. J. Abbott (e-mail: jake.abbott@utah.edu).

Color versions of one or more figures in this article are available at https://doi.org/10.1109/TMAG.2025.3628163.

Digital Object Identifier 10.1109/TMAG.2025.3628163

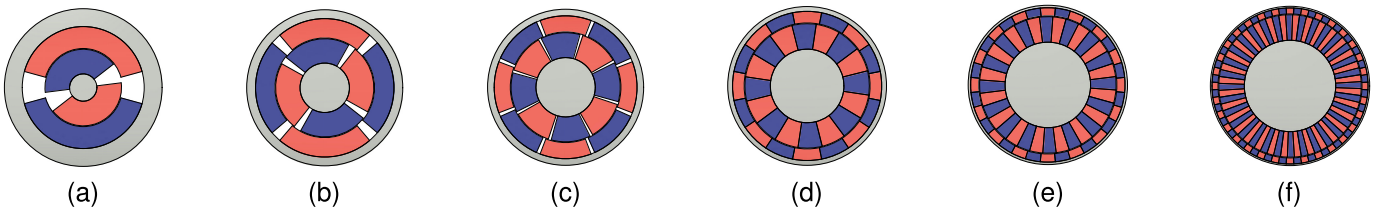

Fig. 2. Schematics depicting results of 2-D-FEA optimization for (a) $Z = 1$, (b) $Z = 2$, (c) $Z = 4$, (d) $Z = 8$, (e) $Z = 16$, and (f) $Z = 32$. Red indicates magnetization radially outward, and blue indicates magnetization radially inward.

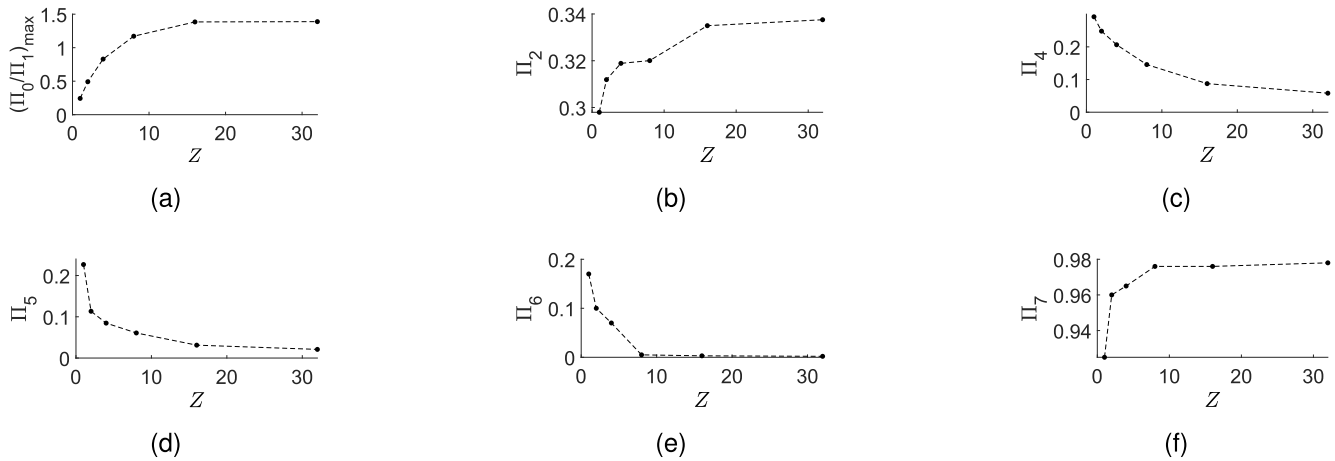

Fig. 3. Results of 2-D-FEA optimization, for each Z considered, for (a) $(\Pi_0/\Pi_1)_{max}$, (b) Π_2, (c) Π_4, (d) Π_5, (e) Π_6, and (f) Π_7.

optimization process. In addition, because any optimization algorithm would trivially drive the air-gap thickness between the IR and OR (i.e., Π_3) to its lower bound, we simply maintain $\Pi_3 = 0.01$ (i.e., 1% of the outer radius, R). It is shown in [1] that small changes to these parameters generally yield small changes to optimal geometric parameters Π_1–Π_7.

The optimization process began with 2-D-FEA simulations, which fundamentally assume $\Pi_1 = L/R \to \infty$. For each of the Z values considered, we created a set of five parameters, Π_2 and Π_4–Π_7, with three levels each, centered on the optimal values for the $Z = 8$ design from [1], which yielded a coarse workspace of 243 designs per Z value. An arbitrary value of $R = 0.3$ m was used in all simulations. A constraint was placed on the algorithm such that

$$d_g + d_m + d_s + d_y \leq R \tag{1}$$

to ensure that the sum of the component widths did not exceed the total radius of the MTC. An arbitrary value of $L = 0.003$ m was used, which has no effect on the results other than being used in the calculation of T/L and thus Π_0/Π_1.

Our process for performing the 2-D simulations is slightly different than that of [1]. The simulations were performed using ANSYS AEDT through the PYAEDT Python interface. Physical geometry parameters were calculated for each simulation and placed into a Maxwell 2-D parametric model that swept the rotor through a full period of each design's waveform in 45 steps and returned the maximum synchronous torque. These simulations utilized the built-in ANSYS TAU meshing algorithm seeded at increasing levels of detail to preserve edge geometry at the higher Z levels. The algorithm includes built-in refinement with a convergence criterion. For the 2-D-FEA simulations, this usually converged within three iterations and always converged within five.

The design parameters yielding the maximum synchronous torque within each Z value were then seeded into a Python gradient-ascent (GA) algorithm. This algorithm was given a convergence tolerance of 1×10^{-5} and a maximum-iterations value of 100. The GA algorithm utilized PYAEDT to simulate each set of design parameters, calculated a gradient for each iteration, and updated the design parameters accordingly. Each Z level converged on a maximum synchronous torque value within 30 iterations. Finally, we transformed the resulting optimal torque-per-length values, T/L, returned in units N, to dimensionless Π_0/Π_1 values based on the optimal independent parameters.

3-D-FEA simulations were used to study the length (i.e., flux-leakage) effects on the optimal 2-D designs. PYAEDT was again utilized to feed the optimal 2-D parameters into a Maxwell 3-D parametric model that swept through seven values of L representing $\Pi_1 \in [0.1, 1.7]$. The adaptive 3-D meshing in ANSYS typically converged within ten iterations and always converged within 15. Finally, we transformed the resulting torque values, T, returned in units N·m, to dimensionless Π_0 values based on the independent parameters. From here, we calculated Π_0/Π_1 based on the particular Π_1 being considered. This enabled us to compare the value of Π_0/Π_1 for finite values of Π_1 to the value of Π_0/Π_1 as $\Pi_1 \to \infty$.

III. Results

The results of the 2-D-FEA optimization process are provided in Figs. 2 and 3, and Table II. The results show clear trends in how optimal design parameters vary with Z. Increasing Z results in an asymptotic increase in the maximum synchronous torque, $(\Pi_0/\Pi_1)_{max}$. Increasing Z causes the yoke, the outer magnets, and the air gap between magnets to get thinner, and the core to get larger, without an appreciable change to the thickness of the inner magnets.

As expected from [1], 3-D-FEA results consistently predict lower torque than the 2-D-FEA results, as shown in Fig. 4, due to flux leakage at the ends of the MTC. As expected, as $\Pi_1 \to \infty$, the differences between the 2-D- and 3-D-FEA results decrease. The previous conclusion in [1] that the 2-D-optimization results are a good approximation for the true 3-D optimum when $\Pi_1 \geq 1$ seems to hold true across values of Z.

TABLE II
RESULTS OF 2-D-FEA OPTIMIZATION, FOR EACH Z CONSIDERED, INCLUDING THE VOLUME FRACTION OF THE PM AND SM MATERIALS

	$Z=1$	$Z=2$	$Z=4$	$Z=8$	$Z=16$	$Z=32$
$\left(\frac{\Pi_0}{\Pi_1}\right)_{\max}$	0.229	0.492	0.830	1.17	1.38	1.39
Π_2	0.298	0.312	0.319	0.320	0.335	0.338
Π_4	0.292	0.248	0.206	0.145	0.0874	0.0582
Π_5	0.227	0.113	0.0847	0.0608	0.0312	0.0210
Π_6	0.170	0.100	0.070	0.005	0.003	0.002
Π_7	0.925	0.960	0.965	0.965	0.976	0.978
PM	0.481	0.624	0.644	0.636	0.622	0.601
SM	0.432	0.314	0.307	0.333	0.349	0.370

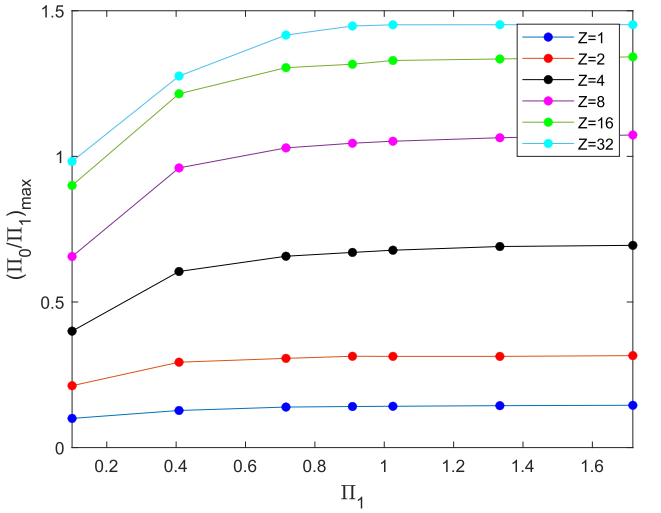

Fig. 4. $(\Pi_0/\Pi_1)_{\max}$ versus Π_1 obtained from 3-D-FEA simulations.

IV. DISCUSSION

Although we only considered $Z \in \{1, 2, 4, 8, 16, 32\}$, one could simply interpolate our results to obtain near-optimal results for other Z values.

We can compare the results of our 2-D optimization at $Z = 8$ to those from [1], which reported $(\Pi_0/\Pi_1)_{\max} = 1.15$ when $\Pi_2 = 0.296$, $\Pi_4 = 0.109$, $\Pi_5 = 0.057$, $\Pi_6 = 0.185$, and $\Pi_7 = 0.978$. We confirm that we achieved nearly the same design, as expected, although we were able to achieve a slightly higher value for $(\Pi_0/\Pi_1)_{\max}$ here. Differences in the optimal design found can be attributed to a lack of sensitivity to certain parameters.

Table II provides the fraction of the total device volume occupied by the two magnetic materials in the optimal designs. The maximum synchronous torque is not trivially tied to the volume of the permanent magnets, due to the need for sufficient flux paths for them to be most effective.

Finally, recall that our optimization assumed Π_3, Π_8, and Π_9 at nominal values. If one were interested in an MTC in which any one of these parameters is substantially different, it would be prudent to run a new optimization, seeded using our optimal parameters. Our choice of $\Pi_3 = 0.01$ represents a rather small air gap, and thus the resulting $(\Pi_0/\Pi_1)_{\max}$ values represent the best we would likely expect to achieve with respect to this parameter; $(\Pi_0/\Pi_1)_{\max}$ will be insensitive to small increases in Π_3, but will decrease rapidly with substantial increases in Π_3. Changing the nominal PM properties used in Π_8 and Π_9 could cause the value of $(\Pi_0/\Pi_1)_{\max}$ to increase or decrease, although we would expect only modest changes when using any comparable grade of NdFeB.

V. CONCLUSION

In this addendum, we applied the design-optimization methodology of [1] to MTCs with 1, 2, 4, 8, 16, and 32 stable equilibria. We observed clear trends in the optimal values of the various MTC parameters as we changed the number of IR/OR magnets, and thus the number of stable equilibria. We also found that the maximum synchronous torque grows asymptotically with the number of stable equilibria, with a diminishing increase (<1%) beyond 16 stable equilibria.

ACKNOWLEDGMENT

This work was supported by the National Science Foundation under Grant 2147765.

REFERENCES

[1] J. L. B. Aman, J. J. Abbott, and S. Roundy, "Optimal parametric design of radial magnetic torque couplers via dimensional analysis," *IEEE Trans. Magn.*, vol. 58, no. 6, pp. 1–8, Jun. 2022.